Electronic Supplementary Material (ESI) for Materials Horizons.

Supporting Information for:

Designing Direct-Indirect Bandgap Transitions in Double Perovskites

T. Thao Tran, [†,§] *Jessica Panella,* [†,§] *Juan Chamorro,* [†,§] *Jennifer R. Morey,* [†,§]

and Tyrel M. McQueen[†,§,‡,*]

[†] Department of Chemistry, Johns Hopkins University, Baltimore, MD 21218, United States

[§] Department of Physics and Astronomy, Institute for Quantum Matter, Johns Hopkins University, Baltimore, MD 21218, United States

[‡] Department of Material Science and Engineering, Johns Hopkins University, Baltimore, MD 21218, United States

CORRESPONDING AUTHOR EMAIL ADDRESS: mcqueen@jhu.edu

Table of contents

Experimental section

Synthesis

Polycrystalline $Cs_2AgSbCl_6$ and $Cs_2AgInCl_6$ were synthesized through solid-state reactions. Stoichiometric amounts of CsF (99.9% Alfa Aesar), AgCl (99.9% Alfa Aesar) and $SbCl_3$ (99.9% Alfa Aesar) (or $InCl_3$) were thoroughly ground and pressed into pellets. The pellets were placed separately in evacuated quartz ampoules that were heated to 210 and 400°C, for $Cs_2AgSbCl_6$ and $Cs_2AgInCl_6$, respectively, held for 5 days, with intermittent re-grindings and then cooled to room temperature at a programmed rate of 180°C h^{-1}.

Polycrystalline $Cs_2AgSb_xIn_{1-x}Cl_6$ ($x = 0.5$, 0.4 and 0.2) was synthesized by mixing stoichiometric amounts of $Cs_2AgSbCl_6$ and $Cs_2AgInCl_6$. The mixtures were separately pressed into pellets. The pellets were placed separately in evacuated quartz ampoules that were heated to 300°C held for 6 days, with intermittent re-grindings and then cooled to room temperature at a programmed rate of 180°C h^{-1}.

Single crystals of $Cs_2AgSbCl_6$ and $Cs_2AgInCl_6$ were grown by hydrothermal techniques. The reaction mixtures of polycrystalline $Cs_2AgSbCl_6$ (4.0 mmol) (or $Cs_2AgInCl_6$ separately) and 12 M HCl (10.0 mL) were placed in 23 mL Teflon-lined stainless steel autoclaves. The autoclaves were closed, gradually heated up to 120 and 160°C, for $Cs_2AgSbCl_6$ and $Cs_2AgInCl_6$, respectively, held for 3 days, and then slowly cooled to room temperature at a programmed rate of 2°C h^{-1}. The solid products were isolated from the mother liquor by vacuum filtration and washed with ethanol. Darkly colored truncated-cubic-shaped crystals and light yellow block-shaped crystals, subsequently determined to be for $Cs_2AgSbCl_6$ and $Cs_2AgInCl_6$, respectively, were obtained in approximately 70 and 60% yields based on starting polycrystalline $Cs_2AgSbCl_6$ and $Cs_2AgInCl_6$.

Structure determination: Single-crystal X-ray diffraction

A dark-green cubic crystal (0.08 × 0.08 × 0.08 mm) ($Cs_2AgSbCl_6$) and a yellow block-shaped crystal (0.08 × 0.08 × 0.08 mm) ($Cs_2AgInCl_6$) were selected for single-crystal diffraction analysis. The data were collected on a Bruker Smart platform diffractometer equipped with a 4K CCD APEX II detector using graphite-monochromated Mo-Kα radiation at -60ºC. A hemisphere of data (1272 frames at 6 cm detector distance) was collected using a narrow-frame algorithm with scan widths of 0.30° in omega and an exposure time of 50 seconds per frame. The data were integrated using the SAINT-V7.23A program,[1] with the intensities corrected for Lorentz factor, polarization, air absorption, and absorption attributable to the variation in the path length through the detector faceplate. SADABS absorption corrections were applied based on the entire data.[1] Redundant reflections were averaged. Final cell constants for $Cs_2AgSbCl_6$ and $Cs_2AgInCl_6$ were refined using 787 and 1141 reflections having $I > 10\sigma(I)$, respectively. The Laue symmetry was determined to be $m\bar{3}m$, and from the systematic absences noted the space group was shown to be either $F432$, $F\bar{4}3m$, or $Fm\bar{3}m$. The crystal structures were determined to crystallize in $Fm\bar{3}m$ space group. The positions of the Ag and Sb (or In) atoms were assigned based on comparison of the metal-Cl distances.

All calculations were performed using SHELXL-97 crystallographic software package.[2] Relevant crystallographic data, selected bond distances and angles, atomic coordinates and equivalent isotropic displacement parameters for $Cs_2AgSbCl_6$ and $Cs_2AgInCl_6$ are given in Tables S1 – S3.

Powder X-ray diffraction

Laboratory powder X-ray diffraction (PXRD) patterns were collected using Cu Kα radiation (λ_{avg} = 1.5418 Å) on a Bruker D8 Focus diffractometer with LynxEye detector. Rietveld refinements of laboratory PXRD data were carried out using TOPAS (Bruker AXS) to determine the crystal structures (Figure S1).

UV-Vis diffuse reflectance and transmission spectroscopy

UV-visible diffuse reflectance data of $Cs_2AgSbCl_6$, $Cs_2AgSb_xIn_{1-x}Cl_6$ (x = 0.5, 0.4, 0.2) and $Cs_2AgInCl_6$ were collected on an Ocean Optics Flame spectrometer equipped w a PX-2 pulsed Xenon light source spectrophotometer over the 300–800 nm spectral range at room temperature with strobe period of 20000 micro-seconds and integration time of 20 ms. UV-visible transmission data were collected on a Cary 60 UV-Vis spectrophotometer over the 200–1100 nm spectral range at room temperature (Figure S9).

Electronic Structure Calculations

The band structure calculations were performed within the local density approximation to density functional theory (DFT-LDA), as implemented in the Elk[3] suite all-electron full-potential linearized augmented-plane wave plus local-orbital (FP-LAPW+LO) code. In addition, to evaluate whether the spin-orbit coupling (SOC) interactions have strong effects on the electronic band structures of these materials, calculations with and without SOC were conducted. For all calculations, a 6 × 6 × 6 k-mesh with the experimentally determined lattice parameters and atomic coordinates were used. For calculations of the phonon density of states (DOS), the internal coordinates were relaxed ($\Delta E < 10^{-4}$ Ha). The finite displacement method with $\Delta = 0.005$ Å and a 2 × 2 × 2 q-point mesh was used to calculate the dynamical matrices from which phonon energy as a function of momentum were calculated. The calculated heat capacity was obtained from integrating phonon DOS:

$$C_v = \int_0^\infty D(\omega)\left(\frac{\omega}{kBT}\right)^2 \frac{1}{e^{\frac{\omega}{kBT}} + e^{\frac{-\omega}{kBT}} - 2}\, d\omega$$

where $D(\omega)$: phonon DOS, ω: frequency, k_B: Boltzmann constant, T: temperature

Photoconductivity measurements

Photoconductivity of a single crystal of $Cs_2AgSbCl_6$ was measured in two-probe, constant voltage mode using the monochromated light source. V_{app} and chopping frequency for this measurement were 1.5 V and 300 Hz, respectively, and temperature is in the range of 10 K – 300 K.

Heat capacity measurements

Heat capacity was measured using the semiadiabatic pulse technique, with three repetitions at each temperature (2 K – 300 K) in a Physical Property Data Measurement system (PPMS, Quantum Design).

Table S1: Crystallographic data

	$Cs_2AgSbCl_6$	$Cs_2AgInCl_6$
M/gmol^{-1}	708.14	701.21
T/K	213(2)	213(2)
λ/ Å	0.71073	0.71073
Crystal system	Cubic	Cubic
Space group	$Fm\overline{3}m$ (No. 225)	$Fm\overline{3}m$ (No. 225)
a/ Å	10.664(3)	10.469(11)
V/ Å^3	1212.9(19)	1147(2)
Z	4	4
D_c/gcm^{-3}	3.878	4.059
μ/mm^{-1}	11.018	11.301
$2\theta_{max}$/°	54.22	54.22
Number of unique reflections	98	98
Number of parameters	8	8
R_{int}	0.0222	0.0179
GOF	1.017	1.440
R(F)[a]	0.0101	0.0067
$R_w(F_o^2)$[b]	0.0258	0.0208
Largest diff. peak/hole (e Å^{-3})	0.219/-0.287	0.253/-0.202

[a] $R(F) = \Sigma||F_o| - |F_c||/\Sigma|F_o|$. [b] $R_w(F_o^2) = [\Sigma w(F_o^2 - F_c^2)^2/\Sigma w(F_o^2)^2]^{1/2}$

Table S2. Selected bond distances (Å) and angles (deg)

$Cs_2AgSbCl_6$		$Cs_2AgInCl_6$	
Ag – Cl × 6	2.706(3)	Ag – Cl × 6	2.724(3)
Sb – Cl × 6	2.626(3)	In – Cl × 6	2.510(3)
Cl – Ag – Cl	90.0, 180.0	Cl – Ag – Cl	90.0, 180.0
Cl – Sb – Cl	90.0, 180.0	Cl – Sb – Cl	90.0, 180.0

Table S3. Atomic coordinates, occupancies and equivalent isotropic displacement parameters (Å^2) for $Cs_2AgSbCl_6$ and $Cs_2AgInCl_6$ from single crystal X-ray diffraction

$Cs_2AgSbCl_6$

Atom	x	y	z	Occ.	U_{eq}[a]	Site
Cs	0.2500	0.2500	0.2500	1.000	0.0302(2)	8c
Ag	0.5000	0.0000	0.0000	1.000	0.0174(2)	4b
Sb	0.0000	0.0000	0.0000	1.000	0.0121(2)	4c
Cl	0.2463(9)	0.0000	0.0000	1.000	0.0343(3)	24a

[a] U_{eq} is defined as one-third of the trace of the orthogonalized U_{ij} tensor

$Cs_2AgInCl_6$

Atom	x	y	z	Occ.	U_{eq}[a]	Site
Cs	0.2500	0.2500	0.2500	1.000	0.0217(2)	8c
Ag	0.5000	0.0000	0.0000	1.000	0.0166(2)	4b
In	0.0000	0.0000	0.0000	1.000	0.0103(2)	4c
Cl	0.2398(9)	0.0000	0.0000	1.000	0.0224(3)	24a

[a] U_{eq} is defined as one-third of the trace of the orthogonalized U_{ij} tensor

Table S4. Atomic coordinates, occupancies and crystallographic sites for $Cs_2AgSbCl_6$, $Cs_2AgSb_xIn_{1-x}Cl_6$ (x = 0.5, 0.4, 0.2) and $Cs_2AgInCl_6$ from Rietveld XRPD refinements

$Cs_2AgSbCl_6$					
Atom	x	y	z	Occ.	Site
Cs	0.2500	0.2500	0.2500	1.000	8c
Ag	0.5000	0.0000	0.0000	1.000	4b
Sb	0.0000	0.0000	0.0000	1.000	4c
Cl	0.2458(6)	0.0000	0.0000	1.000	24a
$Cs_2AgSb_{0.5}In_{0.5}Cl_6$					
Atom	x	y	z	Occ.	Site
Cs	0.2500	0.2500	0.2500	1.000	8c
Ag	0.5000	0.0000	0.0000	1.000	4b
Sb	0.0000	0.0000	0.0000	0.4895(9)	4c
In	0.0000	0.0000	0.0000	0.5105(8)	4c
Cl	0.2541(7)	0.0000	0.0000	1.000	24a
$Cs_2AgSb_{0.4}In_{0.6}Cl_6$					
Atom	x	y	z	Occ.	Site
Cs	0.2500	0.2500	0.2500	1.000	8c
Ag	0.5000	0.0000	0.0000	1.000	4b
Sb	0.0000	0.0000	0.0000	0.4021(7)	4c
In	0.0000	0.0000	0.0000	0.5989(9)	4c
Cl	0.2520(6)	0.0000	0.0000	1.000	24a
$Cs_2AgSb_{0.2}In_{0.8}Cl_6$					
Atom	x	y	z	Occ.	Site
Cs	0.2500	0.2500	0.2500	1.000	8c
Ag	0.5000	0.0000	0.0000	1.000	4b
Sb	0.0000	0.0000	0.0000	0.2069(8)	4c
In	0.0000	0.0000	0.0000	0.7931(6)	4c
Cl	0.2509(8)	0.0000	0.0000	1.000	24a
$Cs_2AgInCl_6$					
Atom	x	y	z	Occ.	Site
Cs	0.2500	0.2500	0.2500	1.000	8c
Ag	0.5000	0.0000	0.0000	1.000	4b
In	0.0000	0.0000	0.0000	1.000	4c
Cl	0.2446(6)	0.0000	0.0000	1.000	24a

Figure S1. Rietveld refinements of the laboratory XRPD patterns for $Cs_2AgSbCl_6$ and $Cs_2AgInCl_6$

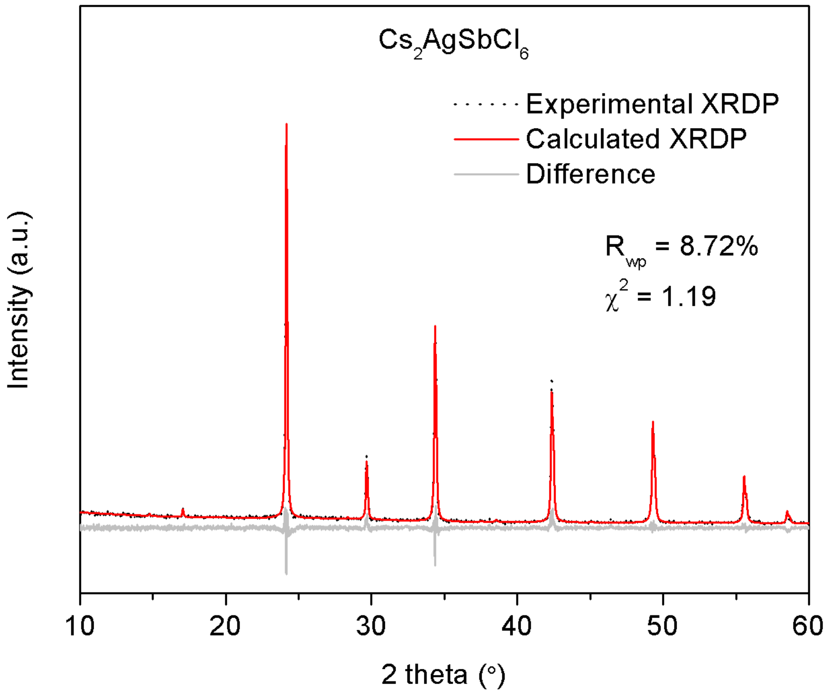

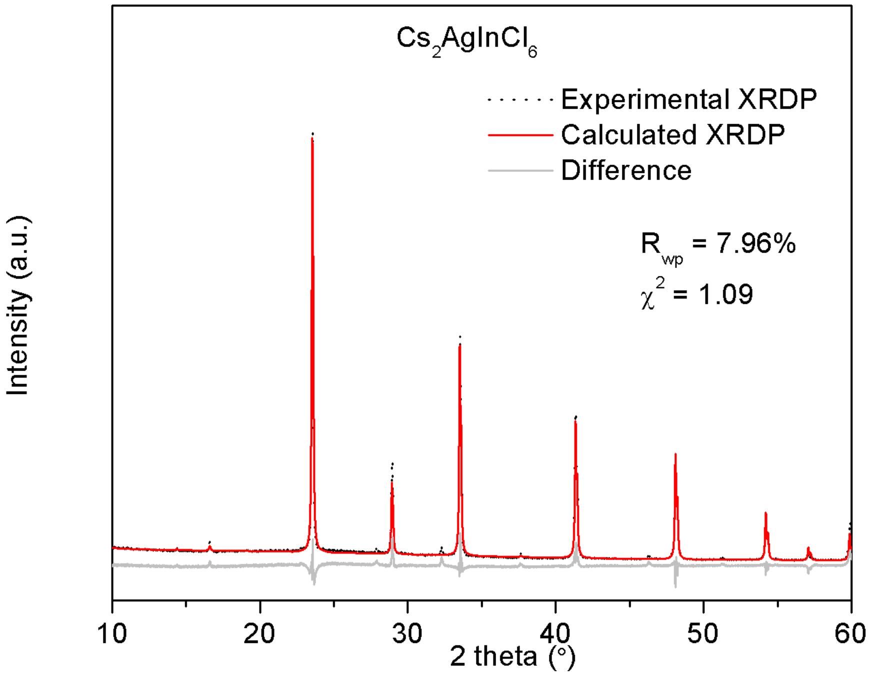

Figure S2. Rietveld refinements of the laboratory XRPD patterns for $Cs_2AgSb_xIn_{1-x}Cl_6$ (x = 0.5, 0.4, 0.2)

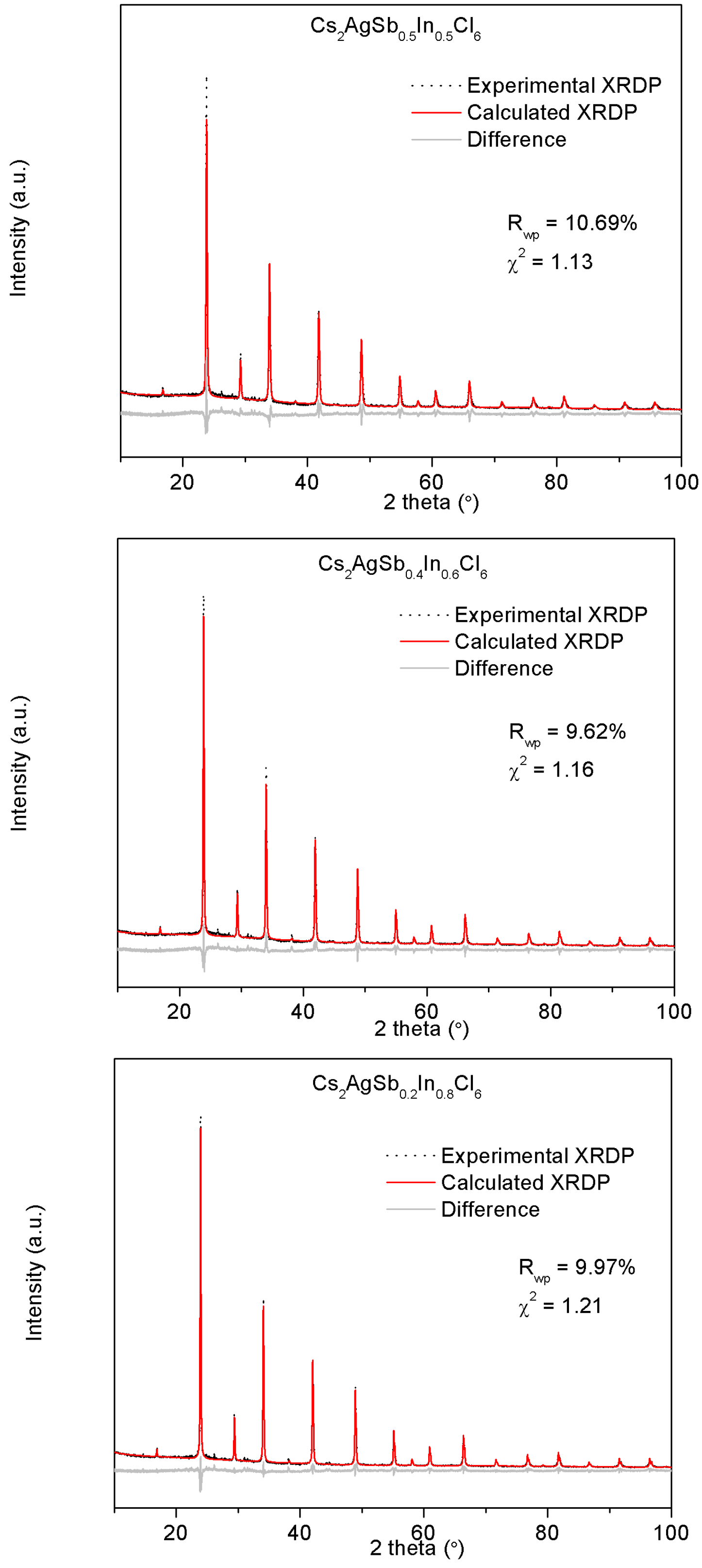

Figure S3. XRPD patterns of $Cs_2AgSbCl_6$, $Cs_2AgSb_xIn_{1-x}Cl_6$ (x = 0.5, 0.4, 0.2) and $Cs_2AgInCl_6$

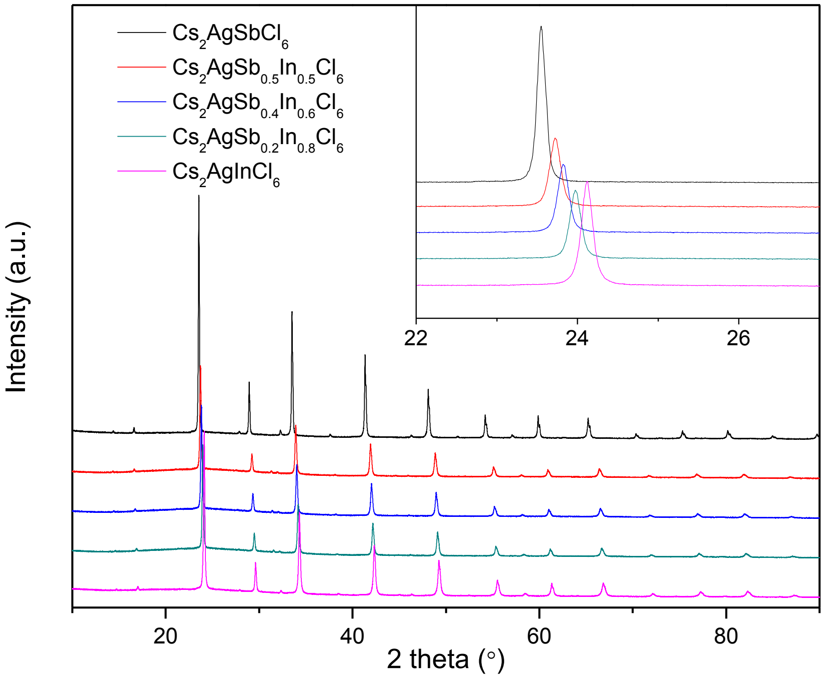

Figure S4. XRPD patterns of $Cs_2AgSbCl_6$ and $Cs_2AgInCl_6$ after 2 – 4 weeks of air and moisture exposure

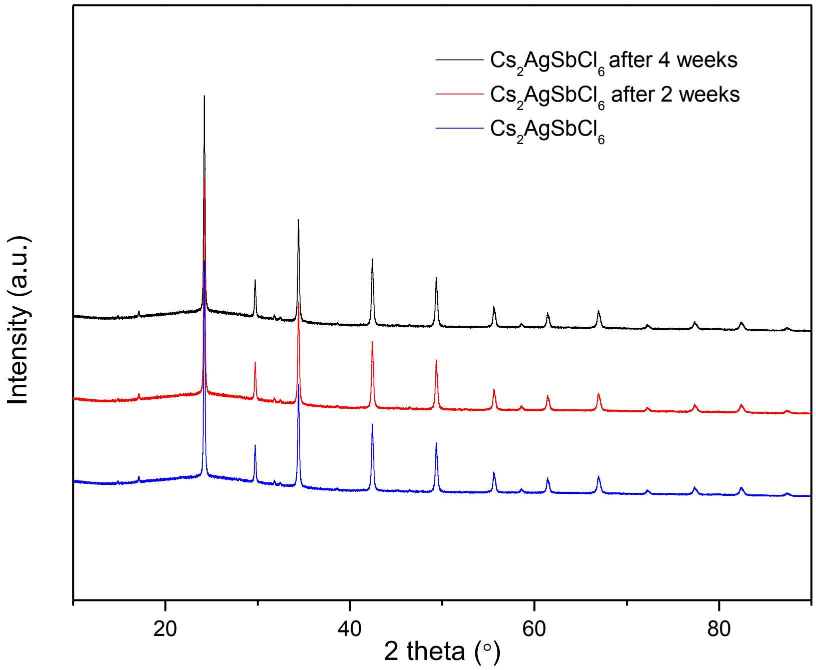

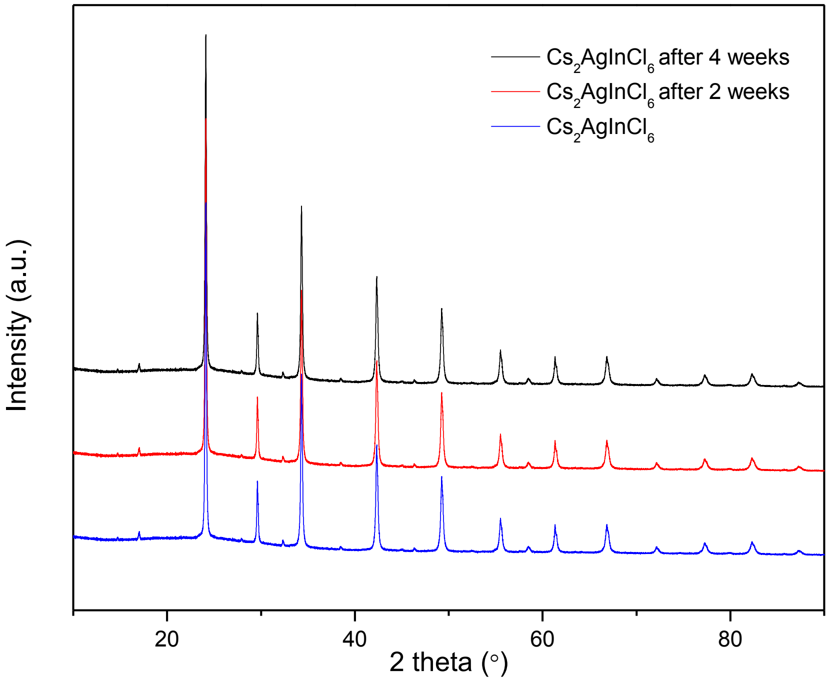

Figure S5. Band structures of $Cs_2AgSbCl_6$ (A) and $Cs_2AgInCl_6$ (B) with and without spin-orbit coupling (SOC). $Cs_2AgSbCl_6$ exhibits a large SOC of 0.6 eV at the Γ (0, 0, 0) point for the first conduction band and has an indirect bandgap with the valence band maximum (VBM) and conduction band minimum (CBM) at the W (π/2a, π/a, 0) and X (0, π/a, 0) points, respectively, of the Brillouin zone. $Cs_2AgInCl_6$ has a direct bandgap with the VBM and CBM both at the Γ (0, 0, 0) point.

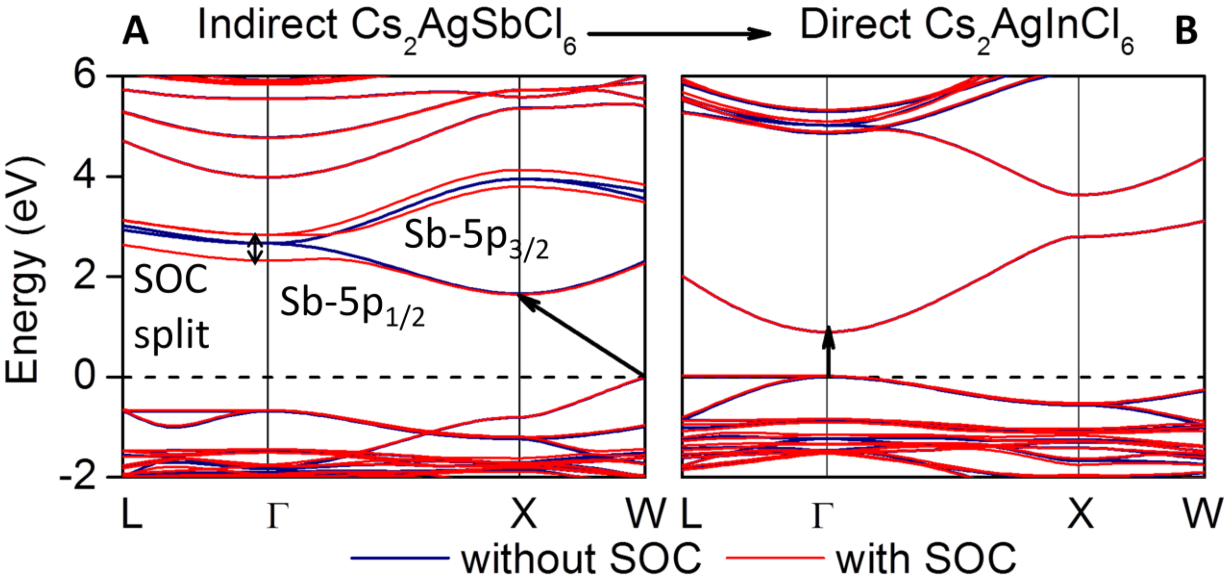

Figure S6. Partial density of states (PDOS) of $Cs_2AgSbCl_6$ and $Cs_2AgInCl_6$

$Cs_2AgSbCl_6$

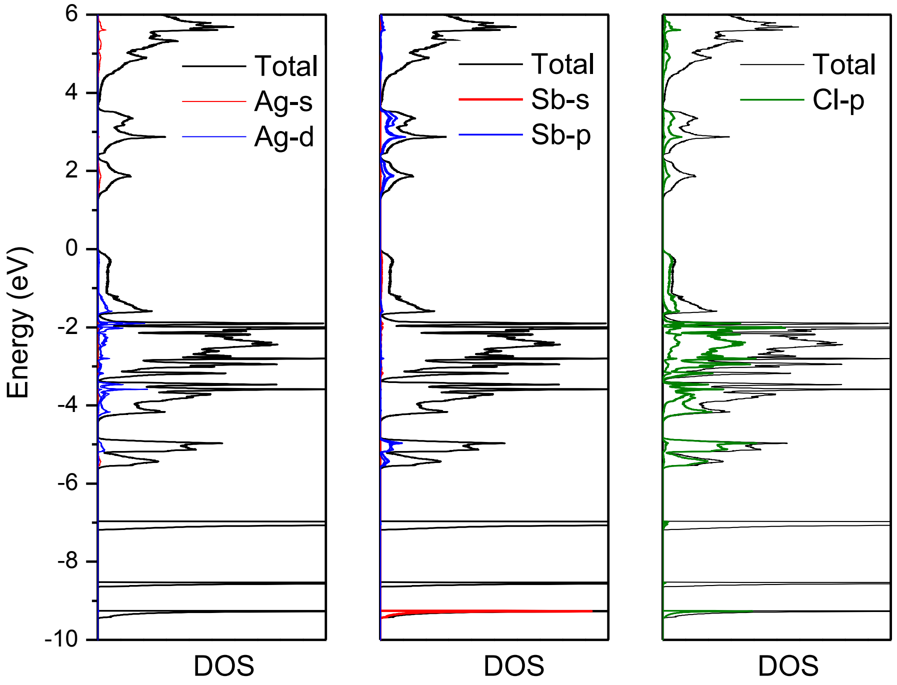

$Cs_2AgInCl_6$

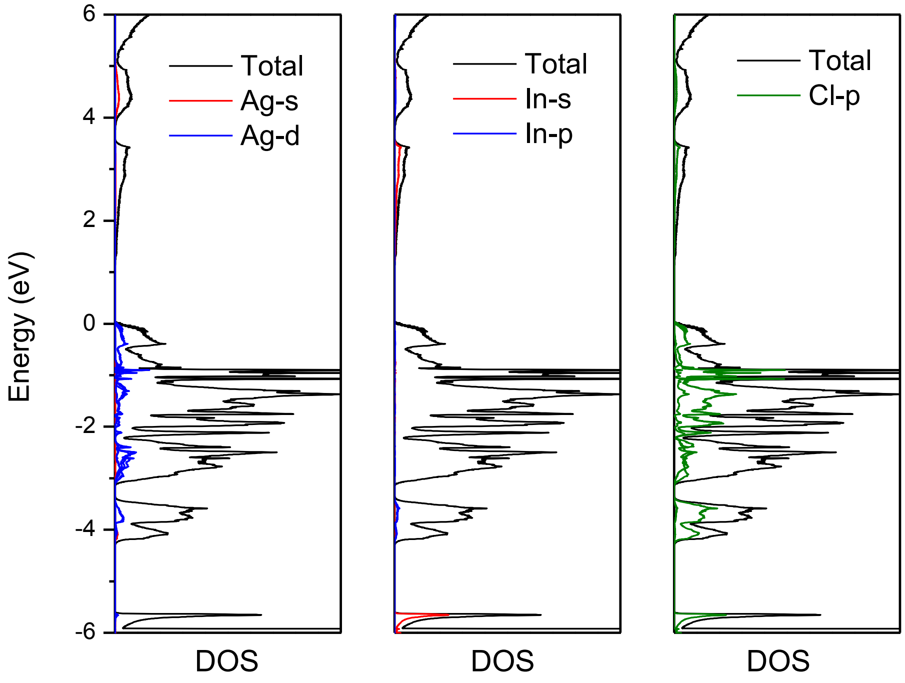

Figure S7. The schematic representation of the bonding and antibonding bands of $Cs_2AgSbCl_6$ (A) and $Cs_2AgInCl_6$ (B). Shaded rectangles correspond to the valence (occupied) bands and white rectangles correspond to the conduction (unoccupied) bands. Note that the valence band maximum (VBM) is predominately antibonding Ag-d/Cl-p states for both perovskites. The conduction band minimum (CBM) is mainly composed of the antibonding Sb-p/Cl-p states (in $Cs_2AgSbCl_6$ (A)) or the antibonding In-s/Cl-p states (in $Cs_2AgInCl_6$ (B))

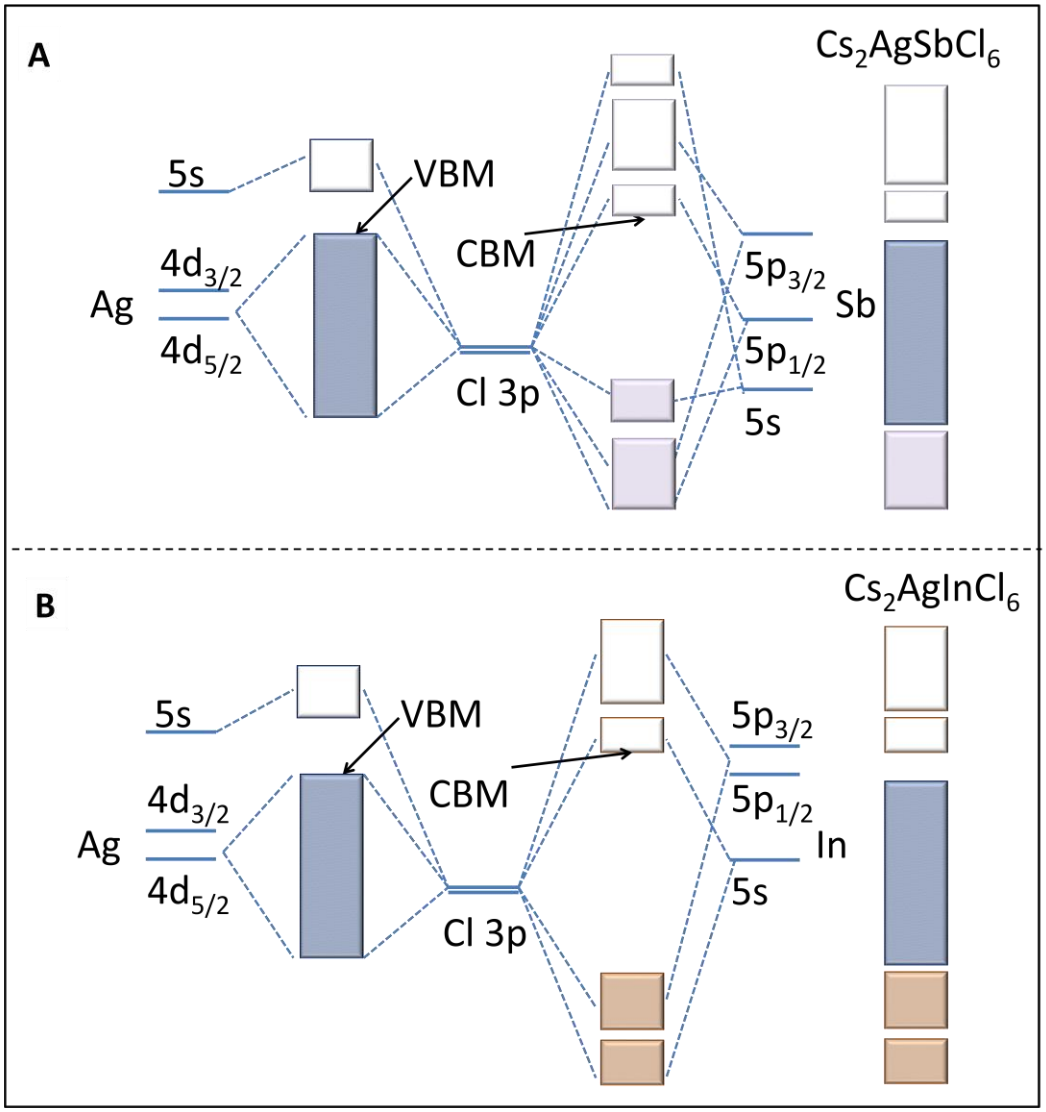

Figure S8. Heat capacity of $Cs_2AgSbCl_6$

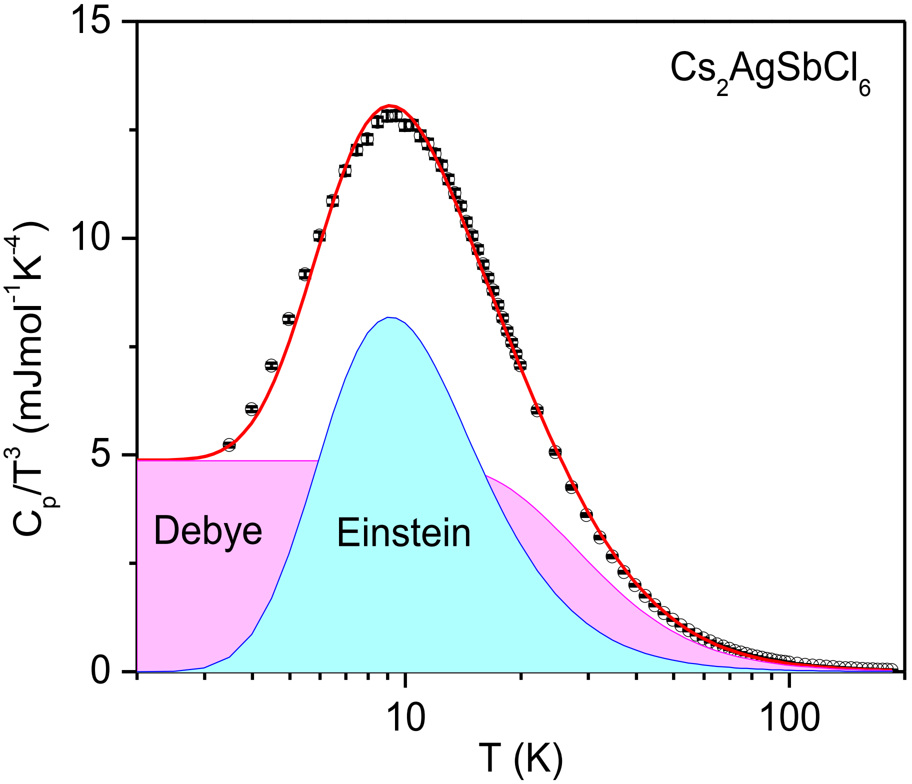

Figure S9. UV-Vis transmission data and Tauc plots for $Cs_2AgSbCl_6$, $Cs_2AgSb_{0.5}In_{0.5}Cl_6$, $Cs_2AgSb_{0.4}In_{0.6}Cl_6$, $Cs_2AgSb_{0.2}In_{0.8}Cl_6$ and $Cs_2AgInCl_6$. The UV-Vis transmission data are consistent with the UV-Vis diffuse reflectance data (Fig. 3).

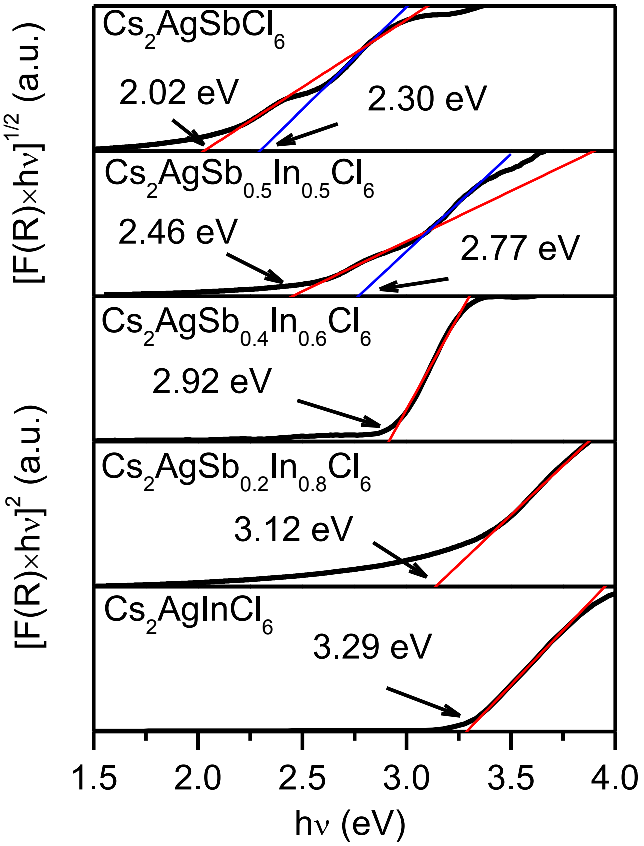

Figure S10. ORTEP representation (50% probability ellipsoids) of $Cs_2AgSbCl_6$ and $Cs_2AgInCl_6$

$Cs_2AgSbCl_6$

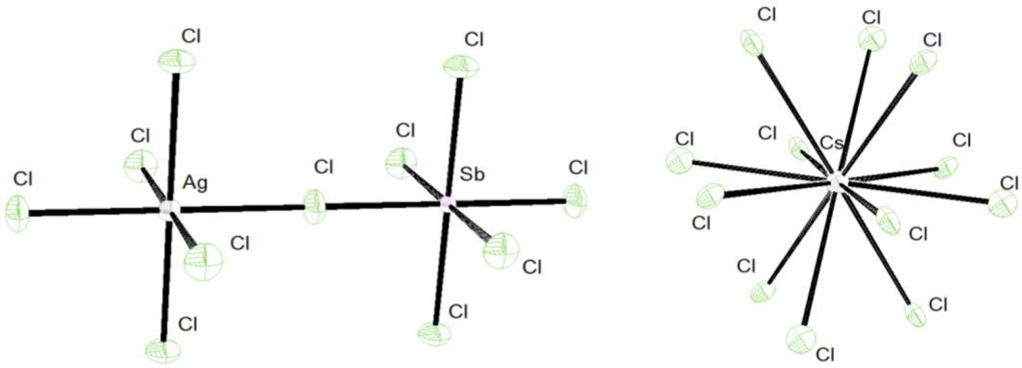

$Cs_2AgInCl_6$

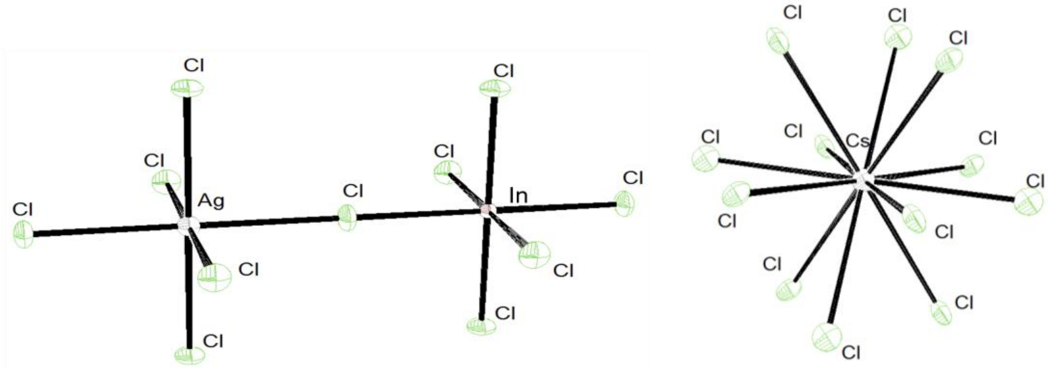

References

(1) SAINT; 7.23A ed.; Bruker AXS Inst. Inc.: Madison, WI: 2005.

(2) Sheldrick, G. M. *Acta Crystallogr., Sect. A: Found. Crystallogr.* **2008**, *64*, 112.

(3) ELKFP-LAPW Code (available at http://elk.sourceforge.net).